An Application of $\mathcal{H}_\infty$ Fault Detection and Isolation to a Transport Aircraft *

Andrés Marcos * , Subhabrata Ganguli, , Gary J. Balas

Department of Aerospace Eng. and Mechanics, 110 Union Street S.E., University of Minnesota, Minneapolis, MM 55455, USA

Abstract

This paper presents an application of $\mathcal{H}_\infty$ fault detection and isolation (FDI) to the longitudinal motion of a Boeing 747-100/200 aircraft. FDI filters are synthesized for open-loop linear, time invariant (LTI) models of the aircraft to detect and isolate faults in the elevator actuator and pitch rate sensor while attenuating the effect of disturbances and noise on the fault signals. Simulations with a nonlinear B-747 aircraft model augmented with a flight controller in the presence of gust and noise validate the fault detection & isolation, the disturbance rejection, and the robust properties of the $\mathcal{H}_\infty$ LTI FDI filters.

Key words: Fault detection, diagnosis and isolation; H-infinity optimization; Aircraft applications

* Research supported under NASA Langley Cooperative Agreement No. NCC-1-337, technical contract monitor Dr. Christine Belcastro.

* Corresponding author. Tel: +1-612-625-6561; Fax: +1-612-626-1558;
Email addresses: marcosa@aem.umn.edu (Andrés Marcos), suvo@aem.umn.edu (Subhabrata Ganguli), balas@aem.umn.edu (Gary J. Balas).

1 Introduction

The fields of fault detection and isolation (FDI) and fault tolerant control (FTC) have attracted much attention from control engineers, especially in the flight control community during the last thirty years. The increased dependency of our modern society on technologically complex systems has given rise to new levels of safety and reliability for these systems not previously considered. The most common approach to provide a system with FDI/FTC functionality is to use hardware redundancy (i.e. duplicate, triplicate, etc the critical software and hardware and use a voting scheme to make a decision as to which component is faulty). The main drawbacks with the hardware redundancy approach is the added complexity and costs resulting from the additional weight and volume of the redundant elements. Another drawback is its un-reliability for components whose outputs are not easily measurable, e.g. actuators. Model-based FDI approaches address those drawbacks by using a mathematical model of the monitored system to make a fault/no-fault decision. Since no mathematical model is exact, robustness to modeling uncertainty becomes a critical issue. Observer-based FDI approaches are the most widespread among the model-based algorithms, and particularly $\mathcal{H}_\infty$-optimization based methods are increasingly of interest due to the issue of robustness of the fault detection and isolation filter.

The basic concepts underlying observer-based FDI schemes are the generation of residuals and the use of an optimal or adaptive threshold function to differentiate faults from disturbances, see (Frank, P.M. and Ding, X., 1997; Patton, R.J. and Chen, J., 1997). Generally, the residuals, also known as diagnostic signals, are generated by the FDI filter from the available input and output

measurements of the monitored system. The threshold function is used to robustify the detection of the fault by minimizing the effects from false faults, disturbances and commands on the residuals. For fault isolation, the generated residual has to include enough information to differentiate said fault from another, usually this is accomplished through structured residuals or directional vectors. Robustness of the FDI algorithm is determined by its capability to de-sensitize the filters from disturbances, errors, and model discrepancies.

In $\mathcal{H}_\infty$-optimization methods, the filtering problem is formulated so that different performance indexes are optimized. The FDI filter has two main design goals: to minimize the influence of non-fault signals (noise, disturbances, uncertainties, commands) on the residuals and to maximize the effects of the faults. These goals are often contradictory since usually a trade-off is required between the residual sensitiveness to faults and its robustness to non-faults. Solutions to the FDI problem using different $\mathcal{H}_\infty$-based techniques have already been proposed: For example, the factorization approach was study in (Ding, X. and Frank, P.M., 1990; Frank, P.M. and Ding, X., 1994); Ricatti-based approach solutions were given to the robust $\mathcal{H}_\infty$ filter problem in (Edelmayer, A., Bokor, J., and Keviczky, L., 1994; Mangoubi, R.S., Appleby, B.D., Verghese, G.C., and Vander Velde, W.E., 1995; Edelmayer, A., Bokor, J., and Keviczky, L., 1996); and the use of an integrated control/filter approach and a standard formulation of the problem were given in (Stoustrup, J., Grimble, M.J., and Niemann, H., 1997).

The importance of this paper is on the application (simulation) of the $\mathcal{H}_\infty$ Ricatti-based LTI FDI technique to a nonlinear system, the Boeing 747-100/200 aircraft, where issues of model uncertainty, realistic disturbances and robustness have to be accounted for in the design stage. Five $\mathcal{H}_\infty$ FDI filters

are developed based on the open-loop aircraft model (i.e. independent from the controller design process) with the main design goal of detecting, isolating, and identifying faults in the longitudinal motion of the Boeing 747 aircraft during closed-loop flight: elevator actuator and pitch rate sensor faults. These five filters are designed at five different equilibrium points using the same interconnection and weights (the latter specifically designed for one of the trim points) in order to study possible strategies to cover the entire flight envelope (e.g. scheduling of filters, linear parameter varying approaches, ...).

2 Literature Survey

A chronological literature survey of $\mathcal{H}_\infty$ FDI applications is provided to further motivate the contribution of this paper. Most of these applications deal mostly with LTI systems where issues of model uncertainty and large deviations from equilibrium are not considered.

In reference (Appleby, B.D., 1990) an LTI application to the estimation of the lateral dynamics of a landing pad with uncertain sea motion using a robust estimator design which parallels the μ-synthesis control design was presented. Extending the previous results to include sensitivity analysis to model uncertainty, reference (Mangoubi, R.S., Appleby, B.D., and Farrel, J., 1992) applied the same algorithm to the simplified longitudinal dynamics of an A4-D aircraft. Noise and wind gust disturbances were represented by the addition of wide-band noise filters for analysis but otherwise the analysis focused on linearized plants that changed with forward velocity. The fault detection factorization approach given in reference (Frank, P.M. and Ding, X., 1994) was applied to an industrial electro-mechanical facility for sensor and actuator faults on

reference (Alcorta García, E., Köppen-Seliger, B, and Frank, P.M., 1995).

A robust failure detection and isolation algorithm based on robust $\mathcal{H}_\infty$ estimation filters was presented in reference (Mangoubi, R.S. et al., 1995) and applied to the open-loop pitch dynamics of an underwater vehicle to detect a single actuator fault. Their analyses were based on open-loop LTI responses where the filters were designed for a nominal condition and tested for a second off-nominal LTI plant for robustness analysis. An empirical evaluation of an estimation algorithm based on $\mathcal{H}_\infty$ filtering techniques was applied in reference (Kawabata, A. and Fujita, M., 1998) to a 2-D visual servoing tracking of a moving target with good results for fast parameters variations.

Focusing on the appropriate selection of the fault reference model (i.e. model matching-based approach) for the robust diagnostic residual generation, (Frisk, E. and Nielsen, L., 1999) gave an example based on a second order DC-servo model with parameter uncertainties. An application of μ-synthesis and D-K iteration using the integrated approach to an inverted pendulum was given in reference (Cardoso, A. and Dourado, A., 1999). The Youla parameterization and the two-degree-of-freedom controller formulation was used in reference (Suzuki, T. and Tomizuka, M., 1999) for an integrated application of a fault detector and controller on a three mass system (LTI simulation, no noise). Reference (Douglas, R.K. and Speyer, J.L., 1999) proposed an approach using the geometric concepts behind the classical fault detectors of (Beard, R.V., 1971; Jones, H.L., 1973; Massoumnia, M.A., 1986) but providing with $\mathcal{H}_\infty$-norm bounding gains and fault enhancement through appropriate performance index. It also provided with an application to a linearized model of the longitudinal dynamics of an F16XL aircraft with fault detection capabilities (accelerometer sensor and elevator faults) and with gust (first-order Dryden filter)

and sensor noise in the simulation environment.

A robust failure detection filter for a reentry vehicle attitude control system was given in reference (Agustin, R.M., Mangoubi, R.S., Hain, R.M., and Adams, N.J., 1999). Their approach was based on dedicated failure detection filters for steady-state, build upon previous work in reference (Mangoubi, R.S. et al., 1995), and in $\mathcal{H}_\infty/\mu$ robust filters for transient fault detection. Nominal LTI filters were synthesized for faults on the aerosurfaces and on the jet thrusts for the lateral dynamics of the Space Shuttle Orbiter and their robustness tested by implementation with an off-nominal LTI plant.

The problem of fault detection was addressed through $\mathcal{H}_\infty$ robust estimator using Popov-Tsypkin multipliers in reference (Collins, E.G. and Song, T., 2000). An application of the approach to a simplified longitudinal flight control system (i.e. short-period dynamics and LTI) with noise and disturbances resulting from Butterworth filters and considering system parameter fluctuations was given. An interesting application to a benchmark system, the three tank problem, of the $\mathcal{H}_\infty$ optimization for the integrated approach was given in reference (Stoustrup, J. and Niemann, H., 2000). Although sparse on implementation details (no interconnection, disturbances inputs or simulation environment) it is quite detailed on its insight on weight selection and problem formulation issues.

A very interesting application of $\mathcal{H}_\infty$ estimation algorithms to aircraft inflight ice detection was given in (Melody, J.W., Hillbrand, T., Basar, T., and Perkins, W.R., 2001). In reference (Ibaraki, S., Suryanarayanan, S., and Tomizuka, M., 2001) it was proposed an approach in which the Luenenberger observer gains from a bank of dedicated Kalman filters are optimized for fault detection

using $\mathcal{H}_\infty$ optimization. An application for the fault management of the lateral control of an automated vehicle was given in that paper with insight on performance weight selection.

A tangential but interesting application of $\mathcal{H}_\infty/\mu$ - FDI techniques is given in (Henry, D., Zolghadri, A., Monsion, M., and Cazaurang, F., 2002) where an off-line fault detection approach is applied to an induction machine. The approach used is an application of frequency domain model invalidation algorithms which relies in the use of the generalized structure value, μ_g, as a residual and threshold indicator. In reference (Felicio, P., Stoustrup, J., Niemann, H., and Lourie, P., 2002) the $\mathcal{H}_\infty$-FDI Ricatti-based approach is used to design fault detection filters for an inverted pendulum. They use parametric linear fractional transformations (LFT) to represent uncertainty and then estimate the parameter uncertainty in order to declare the fault. Unfortunately the application was not fully carried out in this case (i.e. no simulations).

3 $\mathcal{H}_\infty$ Robust Fault Diagnosis Problem

This section presents a brief introduction to the definitions and goals of $\mathcal{H}_\infty$ fault detection and isolation filters. One of the first tasks required to solve a robust fault diagnosis problem in the $\mathcal{H}_\infty$ framework is to provide with a standard formulation. A standard formulation unifies the diverse approaches and provides a systematic methodology for FDI filter design. For simplicity in the presentation, it is assumed a generalized plant is available (actuators, sensors, and weighting functions are embedded in the plant description). This assumption is quite important in practice since the correct weight selection is vital to obtain a meaningful solution of the problem but it does not affect the

theoretical developments presented and simplifies the presentation.

Assume the monitored system is given by equation (1), where the uncertainty is decomposed into additive uncertain terms for the command inputs $\tilde{\Delta}_u$, the faults $\tilde{\Delta}_f$, and the disturbances $\tilde{\Delta}_d$. Note, that this is quite a general representation of uncertainty and might include model or signal uncertainty.

$$y = G_u\ \vec{u} + G_f\ \vec{f} + G_d\ \vec{d} + \tilde{\Delta}_u\ \vec{u} + \tilde{\Delta}_f\ \vec{f} + \tilde{\Delta}_d\ \vec{d} \tag{1}$$

The transfer function G_u determines the effects of the known inputs, $\vec{u} \in \mathcal{R}^{n_u}$, on the system, those from the faults $\vec{f} \in \mathcal{R}^{n_f}$ are given by G_f, and G_d refers to those from the disturbances $\vec{d} \in \mathcal{R}^{n_d}$. These transfer functions are assumed to be known. Figure 1 shows the desired standard $\mathcal{H}_\infty$ robust fault diagnosis formulation.

In order to derive a state-space representation and provide more insight into the problem, the standard problem given in Figure 1 is re-drawn in Figure 2. It is assumed that all the uncertainty descriptions have been lumped into a (structured or unstructured) uncertainty set characterized by $z = \Delta\ w$. An ideal fault model, $T_{f_{id}}$, is included in the spirit of the model-matching approach to adequately estimate the faults. Typically, this reference model is diagonal for fault de-coupling purposes (isolability), and depending on the type of application it can be an identity matrix (Stoustrup, J. and Niemann, H., 2000) or a frequency dependent weight used to emphasized the frequency band of interest (Frisk, E. and Nielsen, L., 1999).

The nominal plant is given by P, and F is the desired stable $\mathcal{H}_\infty$ filter. The vectors $\vec{f}, \vec{d}, \vec{u}$ correspond to the fault, disturbance and control inputs respectively. The estimation error is given by $\vec{e}$, and is the difference between the

fault and the residual vector, $r\vec{e}s$. The output from the plant is given by the $\vec{y}$ vector, and $\vec{w}, \vec{z}$ denote the fictitious inputs and outputs of the uncertain model, Δ. Let $\vec{x}_p$ be the plant state vector, and $\vec{x}_f$ the states for the filter. The augmented plant state-space representation is given by:

$$\dot{\vec{x}}_p = A_p\ \vec{x}_p + B_p\ \vec{u} + E_{p_1}\ \vec{d} + R_{p_1}\ \vec{f} + Q_1\ \vec{z} \tag{2}$$

$$\vec{y} = C_p\ \vec{x}_p + D_p\ \vec{u} + E_{p_2}\ \vec{d} + R_{p_2}\ \vec{f} + Q_2\ \vec{z} \tag{3}$$

where Q_i represents the effects of the uncertainty on the plant and R_{p_1}, R_{p_2} the fault signatures. The filter and estimation error equations are:

$$\dot{\vec{x}}_f = A_f\ \vec{x}_f + B_{f_1}\ \vec{u} + B_{f_2}\ \vec{y} \tag{4}$$

$$r\vec{e}s = C_f\ \vec{x}_f + D_{f_1}\ \vec{u} + D_{f_1}\ \vec{y} \tag{5}$$

$$\vec{e} = T_{f_{id}}\ \vec{f} - I\ r\vec{e}s \tag{6}$$

where all the matrices are of appropriate order. All the system matrices are known except for those corresponding to the filter $(A_f, B_{f_1}, B_{f_2}, C_f, D_{f_1}, D_{f_2})$. The perturbation output, $\vec{z}$, can be considered as a special type of disturbance, (Chen, J. and Patton, R.J., 1999), and combined with the disturbance, $\vec{d}$, to form a generalized disturbance vector, $\bar{d} = [\ \vec{z}\ \ \vec{d}\ ]^\top$. The $\mathcal{H}_\infty$ robust fault diagnosis problem is then given by equations $(2 \rightarrow 6)$ and is defined as finding a stable filter F such that the performance error is minimized in the face of all possible uncertainties defined by $||\Delta|| \leq 1$.

Once the formulation of the problem has been posed in the standard set-up given in Figure 1, an appropriate optimization index must be selected. The general objective of the robust $\mathcal{H}_\infty$ filter synthesis is to find a stable filter that maximizes the faults effect on the errors (i.e. max $||TF_{e\,f}||_\infty$) while

minimizing the transfer function from the disturbances to the errors (i.e min $||TF_{e\,\hat{d}}||_\infty$ where $\hat{d} = [\bar{d}\ \ \vec{u}]$). This multi-objective optimization is not easily amenable for $\mathcal{H}_\infty$ techniques due to its min-max characteristics. The inclusion of the ideal model allows for a more proper blending of the optimization objectives. Maximizing the effect of the faults on the residual is transformed into minimizing the error between the residual and the weighted fault, i.e $max\ ||TF_{e\,f}||_\infty \equiv min\ ||\ res - T_{f_{id}}\ f\ ||_\infty$. The ideal fault reference model is also used to formulate the different problems regarding fault diagnostic: detection, estimation, and isolation, see Refs. (Stoustrup, J. and Niemann, H., 2000, 2002). Fault detection involves a much simpler problem since only the apparition of the fault is required. Fault estimation (isolation and identification are both included) requires knowledge of the magnitude and/or direction of the fault.

A standard performance index can be given as follows:

$$\sup_{0<\Psi<\infty} \frac{||\ \vec{res} - T_{f_{id}}\ \vec{f}\ ||_2}{\Psi} \tag{7}$$

and the terms $T_{f_{id}}$ and Ψ vary depending on the type of problem. For fault detection any of the possibles faults should just trigger a non-zero residual, i.e. $T_{f_{id}} = 1 \times n_f$. For fault estimation-isolation the residuals should only be affected by the corresponding fault (this will be a *de facto* dedicated structured residual), i.e. $T_{f_{id}} = I_{n_f}$. For identification it is required that the size and nature of the fault be measured, which probably requires a combination of the previous two, i.e diagonal matrix with $rank(T_{f_{id}}) = n_f$. The term Ψ simply indicates whether the optimization is being done without disturbance considerations ($\Psi = ||\ f\ ||_2$) or with minimization of the disturbances ($\Psi = ||\ d\ ||_2$).

The solution to this problem in the present paper follows the state-space approach for $\mathcal{H}_\infty$ optimization given in Refs. (Glover, K. and Doyle, J.C., 1988; Doyle, J.C., Glover, K., Khargonekar, P., and Francis, B.A., 1989; Balas, G.J., Doyle, J.C., Glover, K., Packard, A., and Smith, R., 1998), i.e. an output feedback problem solved using the *hinfsyn* Matlab command. These results were originally developed from the optimal control perspective but carry over to the filter problem by a correct posing of the problem. Similar results obtained specifically for the FDI filter problem can be found in Refs. (Edelmayer, A. et al., 1994, 1996; Chen, J. and Patton, R.J., 1999).

4 Aircraft, Turbulence and Controller Models

In this section the aircraft nonlinear and linear time-invariant (LTI) models for the longitudinal axis, the turbulence model, and the controller used are presented. A more detailed presentation of the aircraft nonlinear model can be found in Ref. (Marcos, A., 2001). The LTI models are used in the design stage while the nonlinear model is used in the closed-loop simulations.

The aircraft model used for this application is the Boeing 747 series 100/200. The Boeing 747 is an inter-continental wide-body transport with four fan jet engines designed to operate from international airports. The focus of the application is on the longitudinal motion of the aircraft. A movable horizontal stabilizer with four elevator segments (i.e. two inboards and two outboards) and the four engines thrust are used to control the longitudinal axis motion. The horizontal stabilizer, δ_s, is only used for trimming purposes. Assuming normal operation of the aircraft, the inboard and outboard elevators move together, hence for the purposes of this research the model is assumed to have

only one elevator surface, δ_e.

An accurate representation of the dynamics of an aircraft can be obtained through nonlinear, rigid-body equations. The nonlinear body-axes longitudinal motion of the Boeing 747, not including flexible effects, can be described by the following differential equations:

$$\dot{\alpha} = \frac{[-F_x \cdot s_\alpha + F_z \cdot c_\alpha]}{m \cdot V_{TAS}} + q \tag{8}$$

$$\dot{q} = c_7 \cdot M_y \tag{9}$$

$$\dot{\theta} = q \tag{10}$$

$$\dot{V_{TAS}} = \frac{1}{m} \cdot [F_x \cdot c_\alpha + F_z \cdot s_\alpha] \tag{11}$$

$$\dot{h_e} = V_{TAS} \cdot c_\alpha \cdot s_\theta - V_{TAS} \cdot s_\alpha \cdot c_\theta \tag{12}$$

The longitudinal states are angle of attack α (rad), pitch rate q (rad/s), true velocity V_{TAS} (m/s), pitch angle θ (rad), and altitude, he (m). The aerodynamic forces along the X and Z-axis and the pitching moment are given by F_x, F_z and M_y respectively. The inertial coefficient is given by $c_7 = 1/I_{yy}$ $(1/\text{Kg}/m^2)$ and the cosine and sine by c_α and s_θ.

The aerodynamic forces and moments are defined in terms of dimensionless aerodynamic coefficients $(C_D, C_L, C_Y, C_l, C_m, C_n)$, flight dynamic pressure $\bar{q}$ (N/m^2), reference area S (m^2), and in the case of the moments, the moment-arm (either wing chord $\bar{c}$ (m), or wing span b (m)). The aerodynamic coefficients are provided as look-up tables (LUT) function of a wide set of parameters (angle of attack, true airspeed, sideslip angle, and altitude among others). They are usually referred to the stability axes and transformed to the pertinent coordinate system by performing rotations through Euler an-

gles. The body-axes is selected as the unifying reference frame in this paper. The longitudinal body-axes aerodynamic forces and moments for the Boeing 747-100/200 are given by:

$$F_x = -\overline{q}S\cdot[C_D\cdot c_\alpha - C_L\cdot s_\alpha] + \sum_{i=1,4} Tn_i - mg\cdot s_\theta \tag{13}$$

$$F_z = -\overline{q}S\cdot[C_D\cdot s_\alpha + C_L\cdot c_\alpha] - 0.0436\cdot \sum_{i=1,4} Tn_i + mg\cdot c_\theta \tag{14}$$

$$\begin{aligned} M_y = \overline{q}S\bar{c}\cdot\{C_m - \frac{1}{\bar{c}}[(C_D\cdot s_\alpha + C_L\cdot c_\alpha)\cdot\overline{x}_{cg} - (C_D\cdot c_\alpha - C_L\cdot s_\alpha)\cdot\overline{z}_{cg}] \\ + \frac{\bar{c}\dot{\alpha}}{V_{TAS}}[C_{m_{\dot{\alpha}}} - \frac{\bar{x}_{cg}}{\bar{c}}\cdot C_{L_{\dot{\alpha}}}\cdot c_\alpha]\} + \sum_{i=1,4} Tn_i\cdot zeng_i \end{aligned} \tag{15}$$

The high-fidelity aerodynamic data for the Boeing 747-100/200 aircraft was obtained from Ref. (Hanke, C., 1971). The full set of aerodynamic coefficients was simplified (but retaining the important dynamics) for the filter design stage. Open-loop time simulation comparisons for the reduced and the full model were performed to ascertain its validity. The details of this reduction can be obtained in (Marcos, A., 2001) where the six aerodynamic coefficients were studied. The reduced aerodynamic coefficients for the longitudinal motion are given below:

$$\begin{aligned} C_L = C_{L_{basic}}(\alpha_w, M) + \frac{dC_L}{dq}(he, M)\cdot\frac{q\bar{c}}{2V_{TAS}}\cdot[1.45 - 1.8x_{c.g.}] \\ + K_\alpha(\alpha_w)\cdot[\frac{dC_L}{d\delta_{E_I}}(he, M) + \frac{dC_L}{d\delta_{E_O}}(he, M)]\cdot\delta_E \end{aligned} \tag{16}$$

$$C_D = C_{D_{Mach}}(M, C_L^*) \tag{17}$$

$$\begin{aligned} C_m = C_{m_{basic}}(\alpha_w, M) + \frac{dC_{m0.25}}{dq}(he, M)\cdot\frac{q\bar{c}}{2V_{TAS}} \\ + K_\alpha(\alpha_w)\cdot\frac{dC_{m0.25}}{d\delta_s}(he, M)\cdot\delta_s \\ + K_\alpha(\alpha_w)\cdot[\frac{dC_{m0.25}}{d\delta_{E_I}}(he, M) + \frac{dC_{m0.25}}{d\delta_{E_O}}(he, M)]\cdot\delta_E \end{aligned} \tag{18}$$

The term $C_{L_{basic}}$ is the basic lift coefficient for the rigid airplane at the zero sta-

bilizer angle in free air with the landing gear retracted. $\frac{dC_L}{dq}(he, M)$ measures the change in the basic lift coefficient due to pitch rate q. The effectiveness factor of the horizontal stabilizer and the elevators is given by K_α which corrects the stability terms for the stabilizer, $\frac{dC_L}{d\delta_s} \cdot \delta_s$, and the inboard/outboard elevators, $\frac{dC_L}{d\delta_{E_I}} \cdot \delta_{E_I}$ and $\frac{dC_L}{d\delta_{E_O}} \cdot \delta_{E_O}$. The drag coefficient is determined by $C_{D_{Mach}}(M, C_L^*)$ which accounts for Mach number effects. The rest of the terms are similar except that applied to the pitching moment coefficient C_m.

The longitudinal axis LTI aircraft model used for the filter design has five states : pitch rate q (rad/s), true airspeed V_{TAS} (m/s), angle-of-attack α (rad), pitch angle θ (rad), and altitude he (m). There are three control inputs: elevator deflection δ_e (deg), stabilizer deflection δ_s (deg) (always set to the corresponding trim value) and thrust Tn (N). The measurements available are flight path angle γ (rad), acceleration $\dot{V}$ (m/s^2/g), pitch angle θ (rad), pitch rate q (rad/s), velocity V_{TAS} (m/s), and altitude he (m).

The deflection and rate limits for the elevator are -23 to 17 deg and ± 37 deg/s respectively. For the stabilizer, the position and rate limits are -12 to 3 deg and 0.5 deg/s respectively, see Ref. (Hanke, C. and Nordwall, D., 1970). Taking the rate limits into account, the elevator and stabilizer are modeled as simple first-order transfer functions: $act_{\delta_e} = 37/(s + 37)$ and $act_{\delta_s} = 0.5/(s + 0.5)$ respectively. The engine dynamics are modeled as $act_{eng} = 0.5/(s + 0.5)$ based on the engine transient characteristics provided in Ref. (Hanke, C. and Nordwall, D., 1970).

The time simulation measurements are corrupted by sensor noise and they also include turbulence entering the nonlinear aircraft model through the stability derivatives. Turbulence is a meteorological phenomenon capable of severely

affecting the performance of an aircraft, either by limiting its precise control or by resulting in tremendous ride discomfort and fatigue. In certain situations (e.g. landing, approach, take-off) it might lead to a catastrophic event. A number of common assumptions regarding turbulence are its description as a process with Gaussian distribution, stationary, homogeneous along the flight path, and isotropic in nature.

The implementation of a realistic turbulence model is carried out using two-dimensional auto-covariance functions. These functions represent the statistical properties of the atmospheric turbulence for a two dimensional stationary, homogeneous and isotropic field of flow. It is an enhancement over the typical one-dimensional flow in that the gust velocity changes in the horizontal plane both along the X_{earth} and Y_{earth} axes (the Z_{earth} is considered negligible due to the relative size of the aircraft along this axis). Basically, turbulence is simulated by feeding white noise through stable, minimum-phase Dryden Spectra filters to the system. For the longitudinal (symmetric) and lateral (asymmetric) motions of an aircraft in turbulence the model developed at Delft University of Technology is followed, see Ref. (Mulder, J.A. and van der Vaart, J.C., 1998).

Coloring filters are used in the simulation to achieve a realistic level of noise in the sensor measurements. The sensor dynamics are modeled using low-pass filters with corner frequency K and gain G, i.e. $z = \frac{K}{s+K}(u + G\ w_{n3})$, where u is the plant output and w_{n3} an independent white noise input.Assuming a noise value equal to σ, a cut-off frequency K, and a white noise signal w_{n3} of unit intensity the adequate gain G can be found by a simple substitution, i.e. $G = \sigma\sqrt{(2/K)}$. For the particular aircraft, the Boeing 747-100/200, the values for the corner frequency and desired output power are given in Table 1.

For closed-loop simulations, LTI $\mathcal{H}_\infty$ controllers obtained at the same trim points as the $\mathcal{H}_\infty$ FDI filters are used. The LTI control synthesis is based on the controller design (adapted for $\mathcal{H}_\infty$ control) and weights given in (Ganguli, S., Marcos, A., and Balas, G.J., 2002). The controller objectives are de-coupled tracking of flight-path angle command, γ_c, and velocity command, V_c, with settling times of 15 sec and 45 sec respectively with the elevator surface fully functional, and the rejection of gust disturbances for the Up-and-Away flight envelope. The controller has five measurements available: flight path angle γ (rad), acceleration $\dot{V}$ (m/s^2/g), pitch angle θ (rad), pitch rate q (rad/s), and velocity V_{TAS} (m/s). There are two control outputs: elevator deflection δ_e (deg), and thrust Tn (N). It was mentioned before that the plant inputs included the two controller outputs and a stabilizer input, δ_s (rad). The latter is used for trim purposes and is held constant at the corresponding trim value for the entire simulation.

5 FDI Filter Design

This section presents the design of the $\mathcal{H}_\infty$ FDI filters. First, the formulation of the filtering problem is presented. A detailed description of the weights used to achieve the performance and robustness objectives follows.

The main philosophy behind the filter design formulation for this study is that of model matching with "tracking" (detection for the FDI filter) requirements. The filters must be able to detect and isolate elevator actuator and pitch rate sensor faults (similar to a de-coupled tracking problem from a control point of view) while rejecting disturbances and noise. The faults are assumed to enter the system in an additive manner: e.g. $\delta_e = u_{actuator} + f_a$.

A first assumption was made of selecting as the input channels to the filter those inputs (γ, $\frac{\dot{V}}{g}$, θ, q and V_{TAS}) and outputs (δ_e, Tn) of the controller with the rationale that in a real implementation it would be easier and economically more meaningful to use the available sensors already installed for the control system. With these filter input channels it was possible to obtain an acceptable level of FDI filter performance (as defined by its ability to detect and isolate the faults) for a small neighborhood around the filter design point (hence the robustness of the filter, as defined by its ability to account for plant variations, was poor). Introducing altitude as an additional input to the filter improved the size of the operating envelope at which the filter performed well (it improved its robustness to plant variations). This is reasonable since the more information the filter has of the plant behavior the better its performance, especially since altitude and velocity are the primary parameters that affect plant dynamics.

The selected FDI $\mathcal{H}_\infty$ filtering interconnection is shown in Figure 3. The vector y is formed by the output signals from the plant (i.e. γ, $\dot{V}$, θ, q, V_{TAS} and he); the disturbance vector is given by $\vec{d}$ and consists of noise for each feedback channel. The control inputs are the elevator deflection and thrust, $\vec{u} = [\delta_e \;\; Tn]^\top$. Two faults are modeled, one for the elevator actuator, fa, and the other in the pitch rate sensor, fs, hence $\vec{f} = [fa \;\; fs]^\top$; equivalently the residual vector is given by $\vec{res} = [res_{act} \;\; res_{sen}]^\top$. The uncertainty input and output channels are represented respectively by $\vec{w}$ and $\vec{z}$.

Selection of the weights is one of the most critical steps, through them it is possible to shape the frequency spectrum of the signals and thus make the system (in the present case the filter) behave as desired. The weights are design using the nominal plant obtained at design point 1 in Table 2 with some

corrections to account for variations with respect to the other design points. A multiplicative input uncertainty to the plant is used to account for uncertainty in the augmented plant (plant, actuator and sensors). The uncertainty weights W_{unc} are chosen as constants representing a 50 percent uncertainty at actuator input: $W_{ele_{unc}} = W_{thrust_{unc}} = 0.5$.

The disturbance weights W_{dist} are used to attenuate the noise/disturbance effects on the fault estimation. Typically these weights are high-pass to account for sensor noise at high frequency regions or low-pass for process and accelerometers noise. Since the pitch rate sensor fault is assumed to enter in an additive manner, the q disturbance weight is critical in shaping the response of the FDI filter. Its gain and corner frequencies are found to be directly connected to the response of the sensor residual. This effect is well-known since for faults and disturbances sharing the same frequency characteristics and direction the fault can not be detected or isolated from the disturbance (Niemann, H. and Stoustrup, J., 1997). Figure 4 shows the frequency responses of the disturbance weights given below:

$$W_{\gamma_{dist}} = \frac{0.1}{57.3}\frac{\frac{s}{0.01}+1}{\frac{s}{50}+1} \qquad W_{\dot{V}_{dist}} = 0.1\frac{\frac{s}{0.01}+1}{\frac{s}{50}+1} \tag{19}$$

$$W_{\theta_{dist}} = \frac{0.1}{57.3}\frac{\frac{s}{0.09}+1}{\frac{s}{40}+1} \qquad W_{q_{dist}} = 0.5\ \frac{s+1}{\frac{s}{100}+1} \tag{20}$$

$$W_{V_{dist}} = 0.05\frac{\frac{s}{0.1}+1}{\frac{s}{50}+1} \qquad W_{he_{dist}} = 100\frac{\frac{s}{0.01}+1}{\frac{s}{50}+1} \tag{21}$$

The faults are filtered by W_{fault} before entering the estimation error equation. This is a common approach in $\mathcal{H}_\infty$ FDI techniques akin to the well-known model matching problem in control, see references (Patton, R.J. and Chen, J., 1997; Stoustrup, J. et al., 1997; Stoustrup, J. and Niemann, H., 2000; Zhou,

K., Doyle, J.C., and Glover, K., 1996). These weights are the knobs used by the filter designer to shape the response of the residuals and define the type of problem. Since a condition of the FDI filter is to provide fault isolation, the reference fault weight W_{fault} is a diagonal matrix which emphasizes the de-coupling of the faults on the residuals. The choice of weights is driven by the need to provide good detection characteristics for the residuals and a sufficiently fast response to fault signals. They correspond to a rise time of 3 to 6 seconds for the actuator and sensor residual respectively. The gains are fine tuned after selecting the disturbance weights to eliminate steady-state errors in the fault detection. As mentioned before, the gain for the sensor residual is directly tied to the gain of the pitch rate noise weight. One can achieve faster responses (down to milliseconds) at the expense of the disturbance rejection properties of the filter and increased coupling between the residuals. Hence, there is a direct trade-off between the fault detection time-domain characteristics as rise time and steady-state error (filter performance) and fault disturbance rejection (filter robustness). The reference fault weights are given below, the corresponding frequency responses are shown in Figure 4:

$$W_{act_{fault}} = 2\,\frac{\frac{s}{300}+1}{\frac{s}{2}+1} \qquad W_{sen_{fault}} = 1.25\,\frac{\frac{s}{300}+1}{s+1} \tag{22}$$

The performance weights W_{error} correspond to the estimation errors. Recall, that the estimation error, equation (6), is the difference between the filtered fault and the residual. Further emphasis on the de-coupling of the residuals is achieved by penalizing both performance errors. The estimation error weights parallel the performance weights in the standard control set-up. The idea is to minimize the error at low frequencies and relax the constraints at higher frequencies. Hence low-pass weights are selected for the actuator and sensor

errors. Interestingly, possibly by zero/pole cancellations, it is noticed that the zeros of the weights showed up as poles of the filter and hence they are selected to be sufficiently small to avoid high-frequency poles which make the filter otherwise too sensitive to noise. The selected estimation error weights are shown in Figure 4:

$$W_{act_{error}} = \frac{\frac{s}{30}+1}{\frac{s}{0.3}+1} \qquad W_{sen_{error}} = \frac{\frac{s}{10}+1}{\frac{s}{0.01}+1} \tag{23}$$

6 Analysis and Results

The FDI filter synthesis is based on the Ricatti solution for the $\mathcal{H}_\infty$ control problem given in (Glover, K. and Doyle, J.C., 1988; Doyle, J.C. et al., 1989) (i.e. using the command *hinfsyn* from (Balas, G.J. et al., 1998)). This approach is based on the feasibility solution of two algebraic Ricatti equations whose solutions must be unique stabilizing positive definite matrices with an associated spectral radius of their product less than γ^2. The final number of states for the filter is equal to the total number of states for the formulation (interconnection, weights, plant). The nominal filter design is carried out at point number 1, low speed and low altitude, in Table 2. The same interconnection structure and weights are used to synthesize additional filters at the other points of the table in order to assess the robustness of the (nominal) design weights and the possibility of gain-scheduling the five LTI filters to cover the entire flight envelope. The $\mathcal{H}_\infty$-norm for the LTI FDI filter at design point number 1 is 6.5372, and the filter has 17 states.

The frequency responses of the transfer functions from both faults and the pitch angle disturbance input to the residuals are shown in Figure 5. Al-

though only the θ disturbance to residuals transfer function is shown, other disturbance channels that also show potential coupling effects for the actuator fault residual are ($\gamma,\ q,\ \theta,\ Vtas$). From the perspective of the effects of the faults on the residuals, it is immediately obvious that both residuals will detect the corresponding fault adequately at low frequencies. Unfortunately, there is coupling of the sensor fault to the actuator fault residual at high frequencies. This coupling although probably small will show up on the time simulations as transients. Decoupling of the actuator fault residual from the sensor fault could be increased by using the sensor error weight, $W_{sen_{error}}$, and the sensor reference model, $W_{sen_{fault}}$, to put more stringent bounds at high frequencies. This would affect the sensor fault residual and probably result in increased coupling on the sensor residual by the actuator fault. From the disturbance rejection perspective, it can be expected during time simulations a degraded detection for the actuator fault residual. Specifically, the elevator fault residual will likely be affected at high frequency by the flight path angle, pitch rate, pitch angle and true airspeed. For the sensor fault residuals there are coupling effects due to the pitch angle at high frequency.

The high frequency characteristics of the FDI filters are deemed acceptable for the present case, longitudinal motion of the Boeing 747-100/200. Recall that the controller implemented is designed with the objective of tracking flight path angle, γ_c, and velocity, V_c, commands. For a given flight path angle command and zero velocity command, the controller uses the pitch angle to track the γ_c command by demanding a change of thrust to achieve the change in altitude and keeping the angle of attack to a minimum variation. Since the controller basically controls the flight path angle, hence θ, and the angle of attack is almost unchanged, the high-frequency interaction from these channels

is kept small. It is expected that this set of commands (i.e zero V_c and non-zero γ_c) will have minimal effect on the residuals. On the other hand, the velocity command demands elevator control (with its fast actuator dynamics compared to the thrust actuator) to achieve the desired velocity trajectory while keeping the flight path angle close to zero, i.e. the trim value for steady level flight. This results in the angle of attack and the pitch angle almost equal and inversely proportional to the velocity command (e.g. a positive velocity step command results in a negative step for the α and θ). These controller strategies are characteristic for the longitudinal motion of an aircraft, see page 150 in (Stevens, B. and Lewis, F., 1992). It is observed that changes in the angle of attack affect the actuator fault residual, hence it is expected that velocity commands will be coupled with this residual. The pitch rate in an aircraft of this type is usually close to zero except for some fast transients when standard manoeuvres are performed. Therefore, during time simulations it is expected that the filters will be able to isolate the faults but will have a more difficult task accurately detecting the actuator fault when velocity commands are input to the controller.

For the purposes of time simulation analysis, the open/closed loop is referred to as LTI whenever an LTI plant model is used in the loop and as nonlinear when the nonlinear aircraft model is used. Also, note that for the closed-loop case, whether LTI or nonlinear, the controller is an LTI $\mathcal{H}_\infty$ controller obtained at the same design point as the $\mathcal{H}_\infty$ FDI filter used in the particular simulation.

The LTI behavior of the FDI filters is analyzed first. The theoretical results in reference (Niemann, H. and Stoustrup, J., 1997) show that when there is no model uncertainty the filter in closed loop can be obtained by multiplying

the open-loop filter by the inverse of the sensitivity function (i.e. $F_{closed} = F_{open} \cdot S^{-1}$). The open-loop and closed-loop designs are said to be equivalent for the nominal case. This fact relies on the existence of a separation principle between the controller and the filter for the non-uncertainty case, i.e. the information for the filter synthesis in the nominal case is not affected by the closed loop inclusion of the controller. In the uncertain case this separation principle does not exist, i.e the uncertainty is introduced to the filter through controller feedback, thereby decreasing the information available to the filter. Hence, for the open and closed loop LTI cases, since there are no modeling errors or uncertainties, the responses of the five filters are expected to be very similar.

Figure 6 shows the aircraft responses, inputs and filter residuals (indistinguishable) for the five LTI closed-loop simulations (at the five points given in Table 2). The commands to the controller are a -2 deg γ_c square input from $t = 15$ to $t = 60$ sec, and a square V_c command of 15 m/s starting at $t = 16$ and ending at $t = 130$ sec. The faults considered (the same are used for all time simulations) are not realistic in the sense that is unlikely that a fault in the actuator or the sensor will show this type of behavior. The faults are shown in the bottom plots of Figure 6 by solid lines and correspond to 50 to 140 percent the non-faulty actuator magnitude and up to 300 percent for the sensor fault. This convoluted set of faults is introduced to differentiate the effect of each fault in the plant outputs while testing the coupling between the faults. The residuals responses are almost identical to those for the LTI open-loop (not shown) due to the lack of model uncertainty in the simulations previously discussed. The filters have the desired dynamic behavior: rise times of 3 to 6 seconds, de-coupling of the residuals, detection of the faults, and

rejection of disturbances (in this case the commands). The sensor fault has a negligible coupling effect on the actuator residual as does the actuator fault on the sensor residual.

The five $\mathcal{H}_\infty$ FDI filters are also implemented in the nonlinear closed-loop simulation. In this case the plant is given by the nonlinear equations of motion of the aircraft from Section 4, this enables to test for model discrepancies with respect to the linear plants used in the filter design procedure. To investigate the robustness of each particular FDI filter a manoeuvre is performed that takes the aircraft sufficiently away from the equilibrium design point. Recall that the different filters are synthesized using the same interconnection and weights, which were mainly obtained for the nominal design point number 1. Hence, it is expected that those filters designed at other points than the nominal will result in a less perfect filter detection performance which will likely degrade as their position (velocity and altitude) increases with respect to the nominal values. The manoeuvre performed is a steadily accelerated climb performed by commanding a 3 deg square flight path angle from $t = 15$ to $t = 95$ and a velocity step command of 18 m/s starting at $t = 20$ sec. The disturbance rejection characteristics of the filters are examined using the turbulence model and noisy sensors described in Section 4.

The FDI filter design at point 5 ($he = 7000$ meters and $Vtas = 241$ m/sec) is used to showcase the noisy closed-loop nonlinear time simulations. The nonlinear closed-loop responses of the aircraft with gust and noise for the $\mathcal{H}_\infty$ FDI filter design are shown in Figure 7. The manoeuvre performed, described above, takes the aircraft in this instance one flight level up (from 7000 m up to 8000 m) and accelerates it from 240 m/s to 258 m/s (from Mach=0.77 to Mach=0.84). It is seen that the filter residuals are able to detect and isolate

the fault signatures with a high degree of accuracy rejecting at the same time command inputs and disturbances effects, although the actuator fault residual has degraded capabilities with respect to the sensor fault residual as expected. The jittery behavior of the residuals, mainly due to sensor noise and gust effects, is relatively small and does not prevent the filter from detecting the faults.

It is also mentioned the effects the faults have on the plant and controller outputs, specifically the sensor fault on (q, α, θ and γ) and both faults on the elevator. These effects are natural since sensor faults (moreover such a dramatic pitch rate sensor) affect primarily the controller behavior which uses the pitch rate as one of the feedback channels. This feedback relationship is easily observed on the plant outputs and inputs. The instant the sensor fault enters the system the controller reacts in almost an impulsive manner (i.e. it reacts by commanding a high demand of the elevator in a very short time) which in turn produces high peaks in the θ, q and γ outputs. With respect to the tracking channels, the sensor fault shows a greater effect on the flight path angle γ which is expected since γ_c has a slower response compared to V_c. The actuator fault has a similar effect, although less dramatic, in the plant outputs and also a small noticeable effect on the sensor residual. Reducing the magnitude of the faults substantially reduces the corresponding peaks in the plant outputs and control outputs.

Next, the nonlinear closed-loop aircraft is simulated at the five design points without noise or gust to measure the effect of plant variations on the performance of the FDI filters (all designed using the same nominal weights). Figure 8 shows the nonlinear close-loop aircraft outputs/inputs and residuals for three of the equilibrium points: points one, three and five in Table 2. Points

three and five are the worst detection cases out of the five points. Although it is a dense plot, the main objective is to show the similar behavior for all the simulations and to highlight the residuals behaviour in the face of variations in the plant states. Recall that in the filter design interconnection not all the plant states were used as filter inputs (i.e. the angle of attack was not used). During the simulations it was observed that some of the commands effects on the residuals seemed to be driven by changes on the angle of attack, i.e. the velocity command results in angle of attack variations and hence a degradation in the elevator fault residual. It is probable that by using this channel as an additional filter input the performance of the filters could be improved in the face of plant variations. With respect to the residuals, it is observed that the sensor residual is much more efficient and robust with respect to plant variations. The actuator residual shows good detection capabilities but is clearly more sensitive to plant variations, especially in the high-speed and high-altitude region. This is expected since the final weights were primarily selected for the low-speed, low-altitude condition (point 1).

The effects of plant variations on the filters performance is an inherent limitation of LTI techniques which restrict the performance and robustness characteristics of the filter to a neighborhood of the design point. The filters performance could be improved by using parameter dependent weights to account for plant variations, by more sophisticated techniques such as gain scheduling and LPV synthesis, or by using adaptive thresholds to remove the effect produced by the commands.

7 Conclusions

In this paper, an $\mathcal{H}_\infty$ fault detection and isolation filter technique has been applied to a nonlinear model of the Boeing 747-100/200 aircraft. Analyses of the robustness properties and disturbance rejection capabilities of the $\mathcal{H}_\infty$ LTI filters have been discussed for open-loop and closed-loop simulations. The $\mathcal{H}_\infty$ FDI filters are capable of detecting and isolating faults in the elevator actuator and the pitch rate sensor for a certain neighborhood of the design point. It is observed that the filter performance and robustness characteristics can be improved by adequate selection of the filter inputs or by using frequency parameter dependent weights.

8 Acknowledgments

This research was supported under NASA Langley Cooperative Agreement No. NCC-1-337, technical contract monitor Dr. Christine Belcastro. The authors wish to thank the faculty of the Aerospace department at Delft University in The Netherlands for the availability of the lecture notes on turbulence and the original software for the Boeing 747-100/200 aircraft.

References

Agustin, R.M., Mangoubi, R.S., Hain, R.M., Adams, N.J., 1999. Robust Failure Detection for Reentry Vehicle Attitude Control Systems. Journal of Guidance, Control, and Dynamics 22 (6), 839–845.

Alcorta García, E., Köppen-Seliger, B, Frank, P.M., Dec. 1995. A Frequency Domain Approach to Residual Generation For the Industrial Actuator Benchmark. Control Engineering Practice 3 (12), 1747–1750.

Appleby, B.D., February 1990. Robust estimator design using the h-infinity norm and mu-synthesis. Ph.D. thesis, Department of Aeronautics and Astronautics MIT.

Balas, G.J., Doyle, J.C., Glover, K., Packard, A., Smith, R., June 1998. μ-Analysis and Synthesis Toolbox.

Beard, R.V., February 1971. Failure accomodation in linear systems through self-reorganization. Ph.D. thesis, Department of Aeronautics and Astronautics MIT.

Cardoso, A., Dourado, A., July 1999. Robust Model-Based Fault Tolerant Control of a Mobile Structure - Application to an Inverted Pendulum. In: 7th International Symposium on Intelligent Robotic Systems. Coimbra, Portugal.

Chen, J., Patton, R.J., 1999. $\mathcal{H}_\infty$ Formulation and Solution for Robust Fault Diagnosis. In: 14th Triennial World Congress of IFAC. Beijing,P.R.China, pp. 127–132.

Collins, E.G., Song, T., September 2000. Robust $\mathcal{H}_\infty$ Estimation and Fault Detection of Uncertain Dynamic Systems. Journal of Guidance, Control, and Dynamics 23 (5), 857–864.

Ding, X., Frank, P.M., 1990. Fault Detection via Factorization Approach. Systems and Control Letters 14, 431–436.

Douglas, R.K., Speyer, J.L., January-February 1999. $\mathcal{H}_\infty$ Bounded Fault Detection Filter. Journal of Guidance, Control, and Dynamics 22 (1), 129–138.

Doyle, J.C., Glover, K., Khargonekar, P., Francis, B.A., 1989. State-Space Solutions to Standard H_2 and $\mathcal{H}_\infty$ Control Problems. IEEE Transactions

on Automatic Control 34 (8), 831–846.

Edelmayer, A., Bokor, J., Keviczky, L., 1994. An $\mathcal{H}_\infty$ Filtering Approach to Robust Detection of Failures in Dynamical Systems. In: 33rd IEEE Conference on Decision and Control. Vol. 3. Lake Buena Vista, FL, USA, pp. 3037 –3039.

Edelmayer, A., Bokor, J., Keviczky, L., 1996. $\mathcal{H}_\infty$ Detection Filter Design for Linear Systems: Comparison of Two Approaches. In: 13th IFAC World Congress, San Francisco, CA. Vol. 7f-01(6). pp. 37–24.

Felicio, P., Stoustrup, J., Niemann, H., Lourie, P., May 2002. Applying Parametric Fault Detection to a Mechanical System. In: American Control Conference. Anchorage, AK.

Frank, P.M., Ding, X., 1994. Frequency Domain Approach to Optimally Robust Residual Generation and Evaluation for Model-based Fault Diagnosis. Automatica 30 (5), 789–804.

Frank, P.M., Ding, X., 1997. Survey of Robust Residual Generation and Evaluation Methods in Observer-Based Fault Detection Systems. Journal of Process Control 7 (6), 403–424.

Frisk, E., Nielsen, L., 1999. Robust Residual Generation for Diagnosis Including a Reference Model for Residual Behavior. In: 14th Triennial World Congress of IFAC. Beijing,P.R.China, pp. 55–60.

Ganguli, S., Marcos, A., Balas, G.J., May 2002. Reconfigurable LPV Control Design for Boeing 747-100/200 Longitudinal Axis. In: American Control Conference. Vol. 5. Anchorage, AK, pp. 3612 –3617.

Glover, K., Doyle, J.C., 1988. State-Space Formulae for All Stabilizing Controllers that Satisfy an $\mathcal{H}_\infty$ norm bound and relations to risk sensitivity. Systems and Control Letters 11, 167–172.

Hanke, C., 1971. The Simulation of a Large Jet Transport Aircraft. Volume

I: Mathematical Model. Tech. Rep. NASA CR-1756, The Boeing Company.

Hanke, C., Nordwall, D., 1970. The Simulation of a Jumbo Jet Transport Aircraft. Volume II: Modeling Data. Tech. Rep. NASA CR-114494/D6-30643-VOL-2, The Boeing Company.

Henry, D., Zolghadri, A., Monsion, M., Cazaurang, F., 2002. Fault Diagnosis in Induction Machines Using the Generalized Structured Singular Value. Control Engineering Practice 10 (6), 587–598.

Ibaraki, S., Suryanarayanan, S., Tomizuka, M., December 2001. $\mathcal{H}_\infty$ Optimization of Luenberger State Observers and Its Application to Fault Detection Filter Design. In: IEEE Conference on Decision and Control. Orlando, FL, pp. 1011–1016.

Jones, H.L., August 1973. Failure detection in linear systems. Ph.D. thesis, Department of Aeronautics and Astronautics MIT.

Kawabata, A., Fujita, M., Jun. 1998. Design of an $\mathcal{H}_\infty$ Filter-Based Robust Visual Servoing System. Control Engineering Practice 6 (6), 219–225.

Mangoubi, R.S., Appleby, B.D., Farrel, J., 1992. Robust Estimation in Fault Detection. In: 31th IEEE Conference on Decision and Control, Tucson, AZ. pp. 2317–2322.

Mangoubi, R.S., Appleby, B.D., Verghese, G.C., Vander Velde, W.E., 1995. A Robust Failure Detection and Isolation Algorithm. In: 34th IEEE Conference on Decision and Control, New Orleans, USA. Vol. 3. pp. 2377 –2382.

Marcos, A., 2001. A Linear Parameter Varying Model of the Boeing 747-100/200 Longitudinal Motion. Master's thesis, Department of Aerospace and Engineering Mechanics, University of Minnesota.

Massoumnia, M.A., February 1986. A geometric approach to failure detection and identification in linear systems. Ph.D. thesis, Department of Aeronautics and Astronautics MIT.

Melody, J.W., Hillbrand, T., Basar, T., Perkins, W.R., 2001. $\mathcal{H}_\infty$ Parameter Identification for Inflight Detection of Aircraft Icing: the Time-Varying Case. Control Engineering Practice 9 (12), 1327–1335.

Mulder, J.A., van der Vaart, J.C., 1998. Aircraft Responses to Atmospheric Turbulence. Tech. Rep. Lectures Notes D-4, Delft University of Technology, Delft, The Netherlands.

Niemann, H., Stoustrup, J., Dec. 1997. Robust fault detection in open loop vs. closed loop. In: 36th IEEE Conference on Decision and Control. San Diego, California, pp. 4496–4497.

Patton, R.J., Chen, J., 1997. Observer-Based Fault Detection and Isolation: Robustness and Applications. Control Engineering Practice 5 (5), 671–682.

Stevens, B., Lewis, F., 1992. Aircraft Control and Simulation, 2nd Edition. John Wiley & Sons, Inc.

Stoustrup, J., Grimble, M.J., Niemann, H., Jul. 1997. Design of integrated systems for the control and detection of actuator/sensor faults. Sensor Review 17 (2), 138–149.

Stoustrup, J., Niemann, H., Jun. 2000. Application of an $\mathcal{H}_\infty$ Based FDI and Control Scheme for the Three Tank System. In: IFAC Symposium on Fault Detection, Supervision and Safety for Technical Processes. pp. 268–273.

Stoustrup, J., Niemann, H., July 2002. Fault Estimation - a Standard Problem Approach. International Journal of Robust and Nonlinear Control 12 (8), 649–673.

Suzuki, T., Tomizuka, M., Aug 1999. Joint Synthesis of Fault Detector and Controller Based on Structure of Two-Degree-of-Freedom Control System. In: IEEE Conference on Decision and Control. Phoenix, AZ, pp. 3599–3604.

Zhou, K., Doyle, J.C., Glover, K., 1996. Robust and Optimal Control. Prenticel-Hall, Englewood Cliffs, NJ.

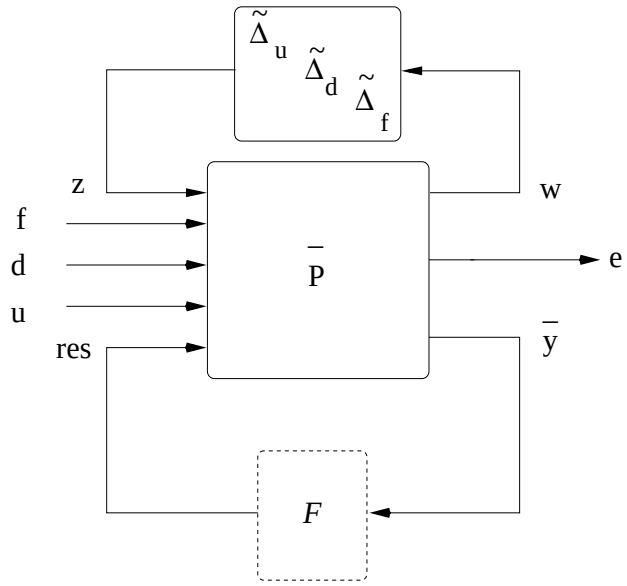

Fig. 1. Standard $\mathcal{H}_\infty$ robust fault diagnosis problem.

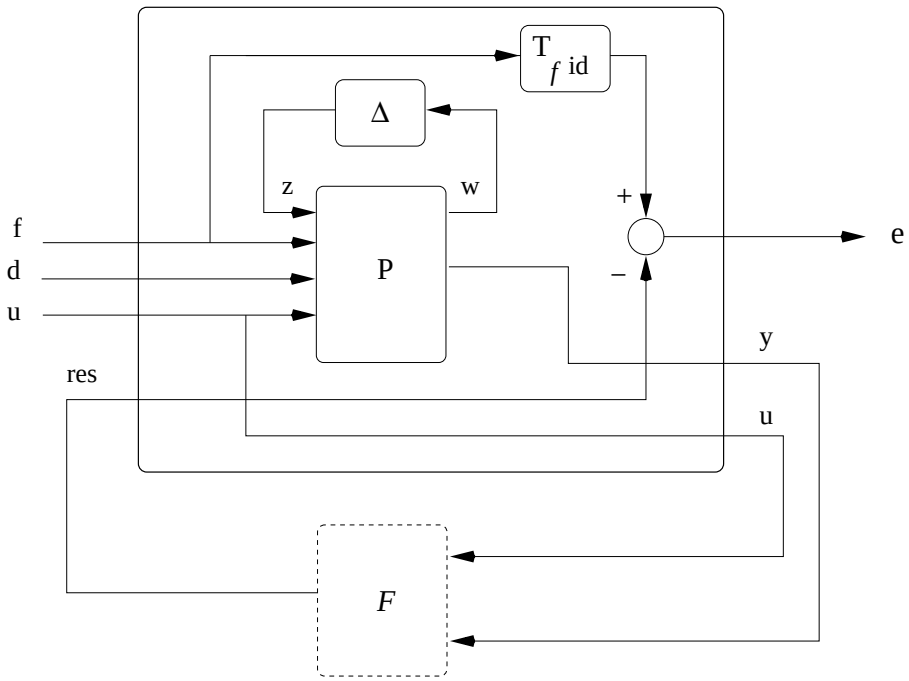

Fig. 2. $\mathcal{H}_\infty$ filter problem with general uncertainty.

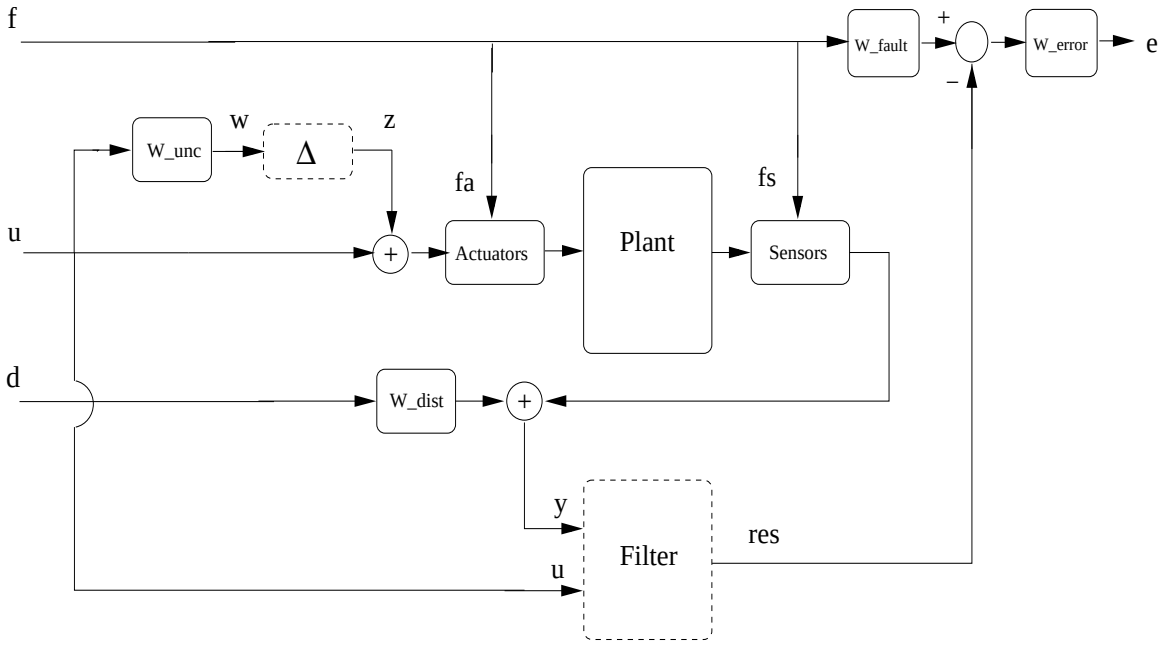

Fig. 3. $\mathcal{H}_\infty$ Filter Interconnection.

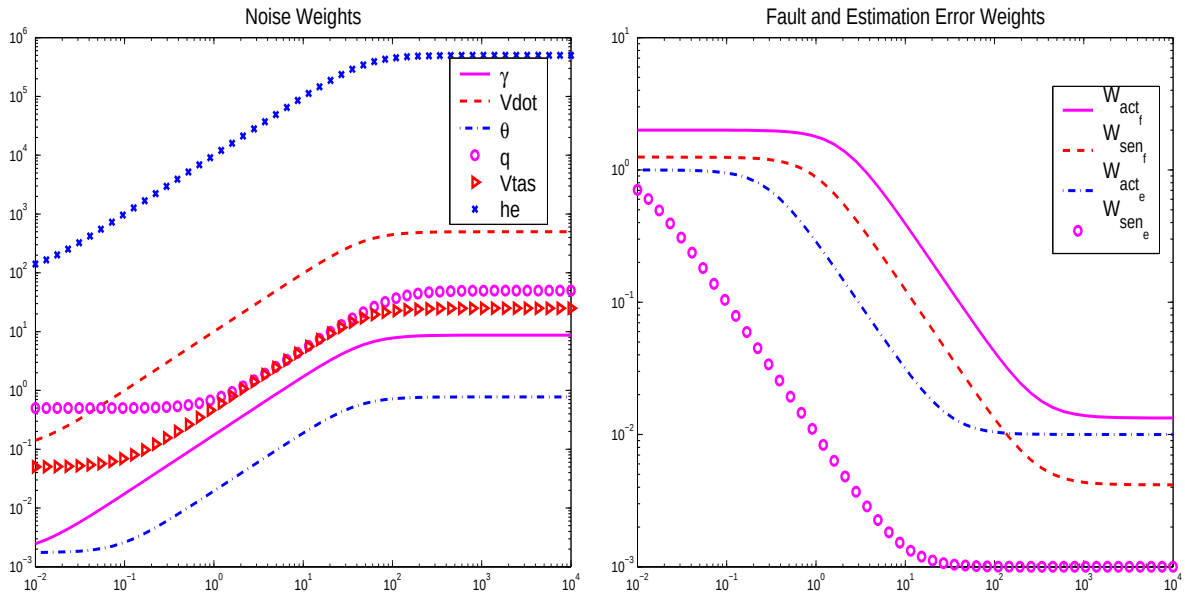

Fig. 4. Disturbance, Filtered Fault and Estimation Error Weights.

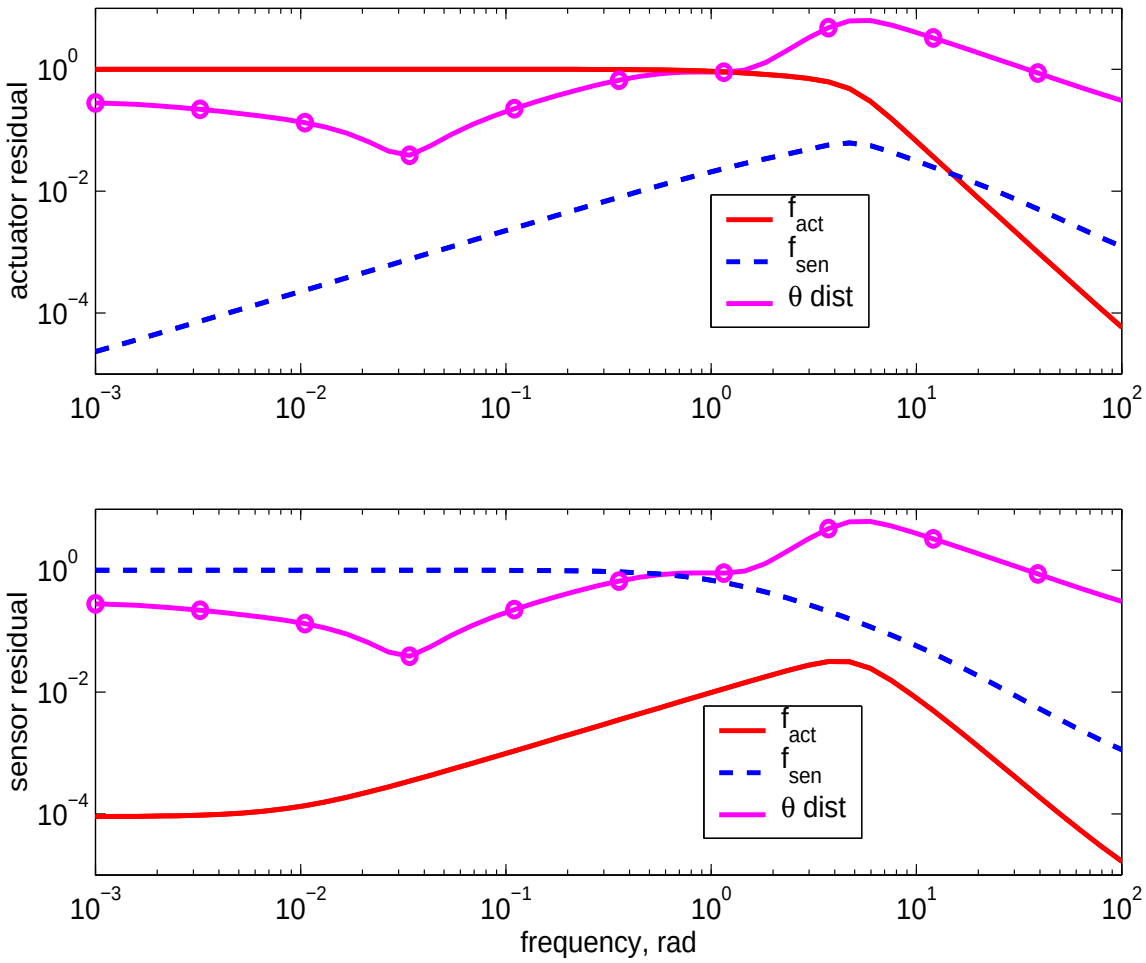

Fig. 5. Frequency response transfer functions faults and disturbances $->$ residuals.

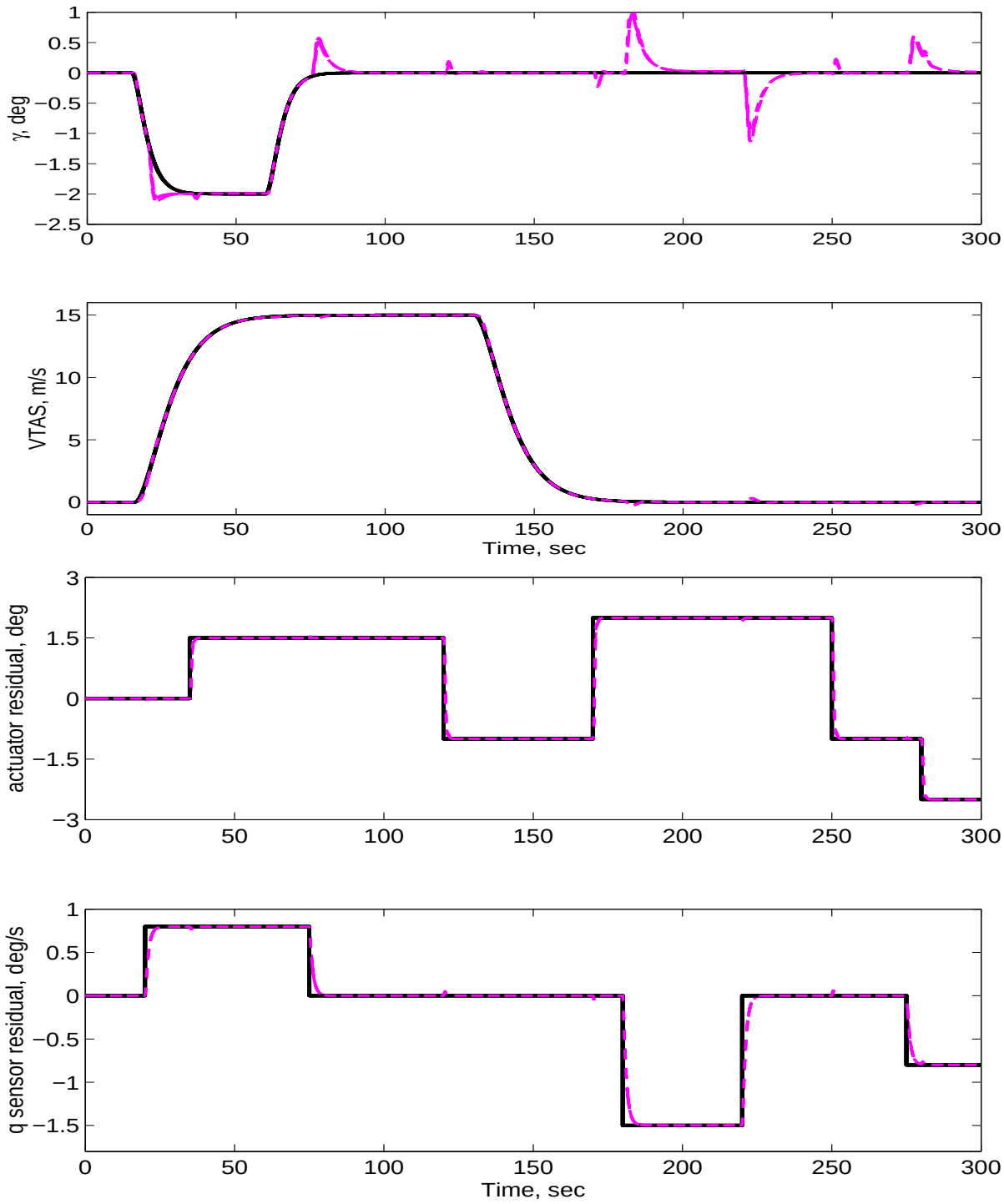

Fig. 6. Plant commands and filter residuals - LTI Closed Loop for all points. Commands/faults (Solid), time responses (dashed)

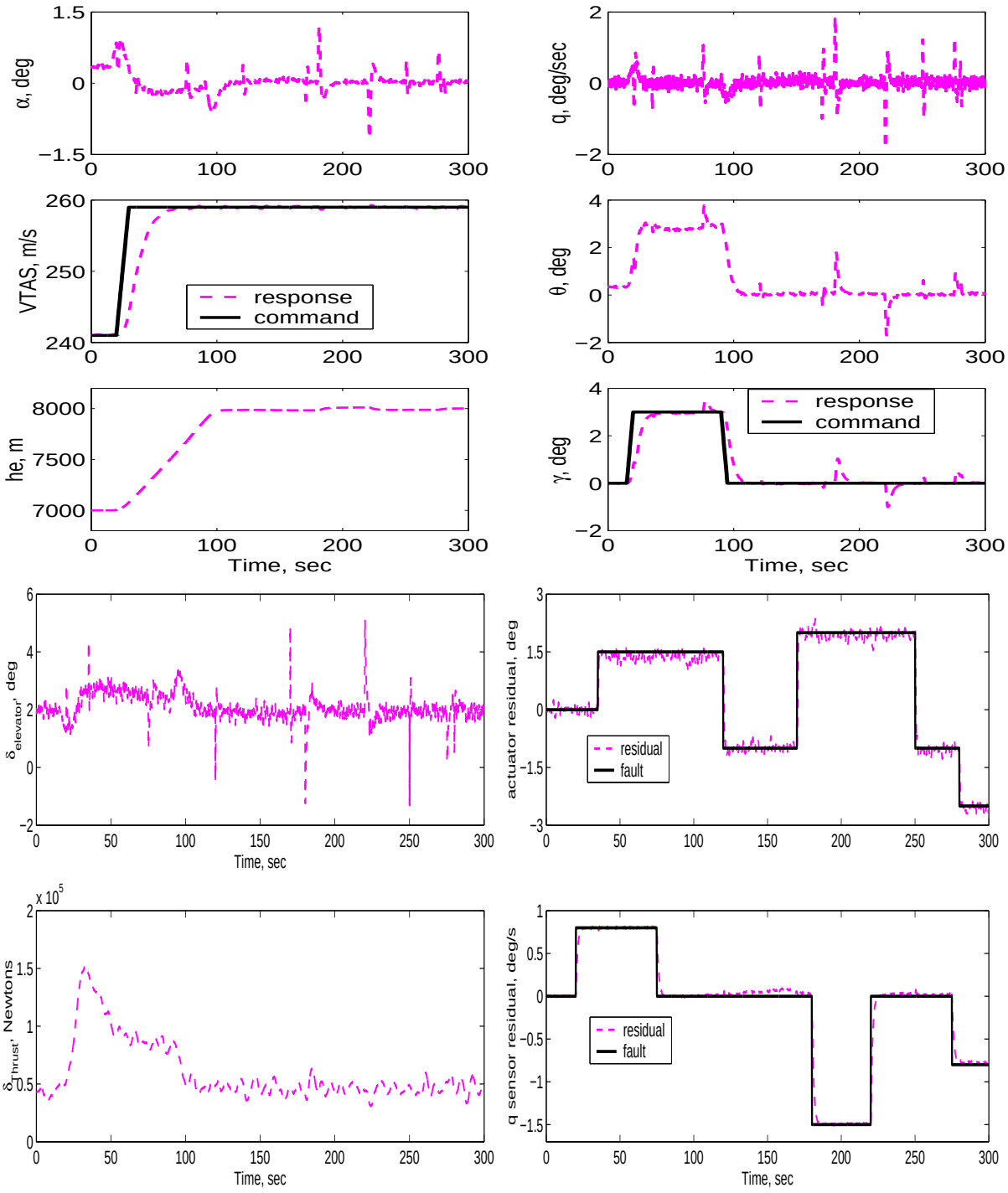

Fig. 7. Plant outputs, inputs and filter residuals - Nonlinear closed loop, moderate gust/noise (point 5).

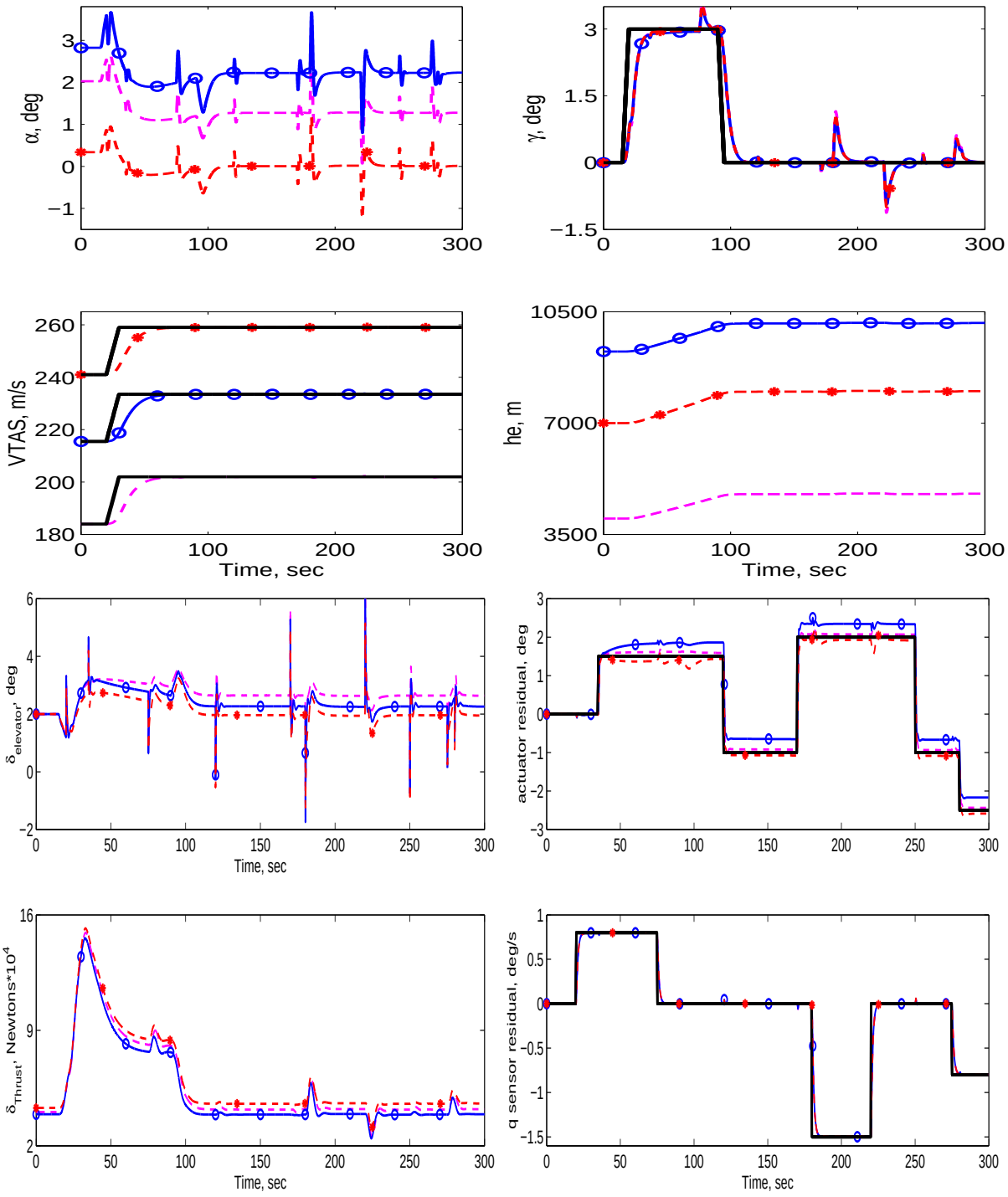

Fig. 8. Plant out/inputs and filter residuals - Nonlinear Closed Loop three points. Commands/faults (Solid), point1 (dashed), point3 (solid with circles), point5 (solid with stars).

Table 1

Sensor noise parameters for the closed-loop time simulations.

sensor	**output power,** σ	**corner frequency,** K
AoA, α	0.1 deg	40 rad
pitch rate, q	0.02 deg	40 rad
pitch angle, θ	0.1 deg	40 rad
normal accel., $\dot{V}/g$	0.1/9.8 m/s^2	40 rad
true airspeed, $Vtas$	0.5 m/s	30 rad
altitude, he	10 m	30 rad

Table 2

Trim points for the Boeing 747-100/200 aircraft.

point	**altitude, m**	**airspeed, m/s**	**Mach number**
1	4000	184	0.567
2	4000	232	0.71
3	9250	125	0.71
4	9250	247	0.81
5	7000	241	0.77